11-2013

Nitroxide-Functionalized Graphene Oxide from Graphite Oxide

Yazmin I. Avila-Vega

Cesar C. Leyva-Porras

Marcela Mireles

Manuel Quevedo-Lopez

Javier Macossay-Torres
The University of Texas Rio Grande Valley

See next page for additional authors

Recommended Citation

Avila-Vega, Y. I., Leyva-Porras, C. C., Mireles, M., Quevedo-López, M., Macossay, J., & Bonilla-Cruz, J. (2013). Nitroxide-functionalized graphene oxide from graphite oxide. Carbon, 63, 376–389. https://doi.org/10.1016/j.carbon.2013.06.093

Authors

Yazmin I. Avila-Vega, Cesar C. Leyva-Porras, Marcela Mireles, Manuel Quevedo-Lopez, Javier Macossay-Torres, and Jose Bonilla-Cruz

Nitroxide-Functionalized Graphene Oxide from Graphite Oxide

Yazmin I. Avila-Vega[a], **Cesar C. Leyva-Porras**[a], **Marcela Mireles**[b], **Manuel Quevedo-López**[b], **Javier Macossay**[c,*], and **José Bonilla-Cruz**[a,*]

[a]Centro de Investigación en Materiales Avanzados S. C. (CIMAV-Unidad Monterrey), Av. Alianza Norte 202, Autopista Monterrey-Aeropuerto Km 10, PIIT, Apodaca-Nuevo León, México, C.P. 66600. Tel/Fax: +52 81 11560809

[b]Department of Material Science and Engineering, The University of Texas-Dallas. 800 W. Campbell, Richardson, TX. 75080, USA

[c]Chemistry Department, The University of Texas-Pan American. 1201 W. University Dr., Edinburg, TX. 78539, USA

Abstract

A facile method for preparing functionalized graphene oxide single layers with nitroxide groups is reported herein. Highly oxidized graphite oxide (GO=90.6%) was obtained, slightly modifying an improved Hummer's method. Oxoammonium salts (OS) were investigated to introduce nitroxide groups to GO, resulting in a one-step functionalization and exfoliation. The mechanisms of functionalization/exfoliation are proposed, where the oxidation of aromatic alcohols to ketone groups, and the formation of alkoxyamine species are suggested. Two kinds of functionalized graphene oxide layers (GOFT1 and GOFT2) were obtained by controlling the amount of OS added. GOFT1 and GOFT2 exhibited a high interlayer spacing (d_{0001} = 1.12nm), which was determined by X-ray diffraction. The presence of new chemical bonds C-N (~9.5 %) and O-O (~4.3 %) from nitroxide attached onto graphene layers were observed by X-ray photoelectron spectroscopy. Single-layers of GOFT1 were observed by HRTEM, exhibiting amorphous and crystalline zones at a 50:50 ratio; in contrast, layers of GOFT2 exhibited a fully amorphous surface. Fingerprint of GOFT1 single layers was obtained by electron diffraction at several tilts. Finally, the potential use of these materials within Nylon 6 matrices was investigated, where an unusual simultaneous increase in tensile stress, tensile strain and Young's modulus was observed.

1. Introduction

Graphene is composed of a single layer of carbon atoms bonded together, which form a two-dimensional hexagonal lattice.[1] This material has attracted great attention from the scientific and technological community due to its unique thermal,[2] electronic[3],[4] and mechanical properties,[5] and is expected to revolutionize many technological fields. The exponential development of methodologies to produce single, or a few layers of graphene has produced significant scientific advancements to date. Graphene can be obtained by: i) micromechanical cleavage,[6] ii) epitaxial growth of graphene films,[7] and iii) chemical processing involving graphite oxidation-intercalation/exfoliation-reduction.[8],[9] However, chemical processing of graphite and derivatives seem to be the most promising methods to

*Corresponding authors: jose.bonilla@cimav.edu.mx; (J. Bonilla-Cruz); jmacossay@utpa.edu (J. Macossay).

obtain single or a few layers of graphene at large-scale, with the most studied methodology of this type being the reduction of graphene from graphite oxide (GO).[9]

Therefore, several ingenious methodologies have been developed to modify the surface of graphite oxide flakes or layers of graphene oxide by attaching functional organic groups to increase their dispersability in common organic solvents, and thus achieve relatively good dispersions[10] in a polymer matrix. Indeed, it is well known that the key for obtaining composites with improved chemical, physical or mechanical properties lies in the use of functionalized nanomaterials[11],[10] (nanoparticles, graphene layers, etc.) and that the choice of functional groups, as well as the control of their concentration onto graphene oxide layers is crucial for the development of advanced materials with unusual properties. On this basis, some fundamental questions have not been answered, such as how is the amount of functionalized organic groups onto graphene layers controlled? What is the critical molar concentration of the functional organic groups attached to graphene layers that allows obtaining a composite with improved properties? Is there any chemical compatibility between the functional organic groups and the polymeric matrix?

On the other hand, nitroxyl radicals (*e.g.* 2,2,6,6-tetramethyl-piperidine-N-oxyl, also known as TEMPO) are stable free radicals extensively used as control agents in the controlled radical polymerization (CRP) of styrenic and some acrylic monomers, in which well-defined polymers with narrow molecular weight distributions are produced.[12] Furthermore, nitroxyl radicals in the presence of a counter-ion can form oxoammonium salts[13] (OS), which have been widely used in the oxidation of primary and secondary alcohols to aldehydes and ketones respectively,[14] via a catalytic process that involves *in situ* generation of the oxoammonium cation through a one-electron oxidation of a nitroxide molecule.[15] In addition to these reactions, we have found that silanol groups (Si-OH) present on the surface of silica dioxide[16] or at the ends of hydroxyl-terminated polymers[17] can be chemically modified with TEMPO groups using OS, promoting a functionalization reaction instead of an oxidation. Recently, Chen *et al.*[18] applied this strategy to functionalize magnetite nanoparticles with TEMPO moieties. To the best of our knowledge, OS have not been studied as intercalating agents to functionalize and exfoliate the groups present on the surface and edges of GO.

Hence, this work reports a scalable, new and simple approach to produce in a one-step synthesis, single layers of graphene oxide decorated with TEMPO moieties (GOFT), using for the first time OS (Br-TEMPO) as intercalating-reaction-compatibilization agents under mild reaction conditions. Two kinds of functionalized graphene oxide layers (GOFT1 and GOFT2) were obtained by controlling the amount of OS added in order to offer some answers to the questions posed previously. To evaluate their potential applications, these materials were incorporated into poly(ε-caprolactam) (Nylon 6) through electrospinning. The resulting non-woven composite nanofibers (GOFT1) presented a ~ 100 % simultaneous increase in tensile stress, tensile strain and Young's modulus in respect to pure Nylon 6 nanofibers. This was an unexpected result and was not observed when GO or graphite sheets were added under the same electrospinning conditions.

2. Experimental

2.1. Materials

Natural graphite platelets (GN, OCF97) were purchased from Superior Graphite, Nylon 6 (Zytel 7301 NC010, MW = 33,300 Da) was kindly provided by DuPont. 2,2,6,6-tetramethylpiperidine-1N-oxyl (TEMPO, $C_9H_{18}NO$, M.W. = 156.25 g/mol, 99 %), N,N,N-triethylamine (Et$_3$N, M.W. = 101.19 g/mol, 99.5 %), bromine (Br$_2$), phosphorus pentoxide (P_2O_5), carbon tetrachloride (CCl_4), dimethylformamide (DMF) and dichloromethane

(CH$_2$Cl$_2$), were purchased from Sigma-Aldrich and used without further purification. 1,1,1,3,3,3-hexafluoro-2-propanol (HFIP, 99.5 %) was acquired from ACROS.

2.2. Instrumentation

The interlayer distance of each sample was analyzed by power X-ray diffraction (XRD, Panalytical Empyream), 5° 2θ 80°, 10.16 s, 0.0167113 s, using Bragg- Brentano geometry. Chemical bonds and composition on the surface and edges were analyzed using X-ray photoelectron spectroscopy (XPS, Perkin-Elmer PHI 5600 ESCA System) using an Al source, k-alpha (1486.7 eV). FTIR-ATR spectra were recorded with a Nexus 470 Spectrometer at 4000–500 cm^{-1} using 32 scans and 4 cm^{-1} of resolution. High-resolution Transmission Electron Microscopy (HRTEM) experiments were performed in the National Laboratory of Nanotechnology at CIMAV using a JEOL JEM-2200FS equipped with a spherical aberration corrector in the condenser lens, and operated at an accelerating voltage of 200 kV. Under these conditions, no visible sample damage was observed during HR-TEM image acquisitions. Scanning electron microscopy (SEM) using an EVO® LS10 (Carl Zeiss Microscopy) was utilized to investigate the electrospun nanofibers morphology. The samples were coated with a thin layer of silver-palladium for 180 s at 45 mA with a Desk II Denton Vacuum Cold Sputter. After coating, the micrographs were taken at an accelerating voltage of 10.75 KV. A 500 watt ultrasonic processor (Sonics Vibra-cell model VCX 500) operating at 20 kHz with an amplitude of 20 % was used for the dispersion of functionalized graphene layers with TEMPO moieties in the polymer solution. A custom made electrospinning chamber consisting of a 10 mL glass syringe with a 22 needle gauge (0.7 mm OD × 0.4 mm ID) at a flow rate of 0.02 mL/min, which was controlled using a KDS 210 pump (KD Scientific Holliston, Inc., MA). High power voltage supplies (ES30P-5W and ES30N-5W for positive and negative voltages, respectively) were purchased from Gamma High Voltage Research (Ormond Beach, FL). The mechanical behavior of the nanofiber mats was investigated using an INSTRON® tensile tester 5943 with a 25 N maximum load cell.

2.3. Synthesis of Oxoammonium Salt (Br-TEMPO)

[16],[17] Bromine (1.64 mL, 0.032 mol) carefully measured using a glass syringe was added slowly to a solution of TEMPO (5 g, 0.032 mol in 100 mL of anhydrous CCl$_4$). A brown solid (Br-TEMPO) was formed instantaneously, isolated and purified using a soxhlet extraction system utilizing CCl$_4$. The Br-TEMPO salt was dried over vacuum at room temperature overnight (yield = 98%). ^{1}H-NMR (CDCl$_3$): δ(ppm): 2.3–2.7 (m, 6H), 1.7–2.0 (s, methyl, 12H).

2.4. Synthesis of GO from GN using an improved Hummer's method

We slightly modified the strategy reported by Marcano *et al.*[19] to obtain GO from GN flakes using an improved Hummer's method. Briefly, a 9:1 mixture of concentrated H$_2$SO$_4$:H$_3$PO$_4$ (360:40 mL) was placed into a 1.5 L glass reactor equipped with a cooling jacket, a condenser and a magnetic stirrer in the presence of a mixture of GN (3 g) and KMnO$_4$ (18 g). Then, the reaction was heated to 50 °C and stirred for 24 h. The reaction was cooled down to 2 °C followed by addition of 3 mL of H$_2$O$_2$ at 30 wt. % under stirring. After that, the reaction system was diluted with deionized water to reach pH = 1 and was filtered using a Nylon membrane of 0.2 μm under vacuum. A dark brown pasty solid was isolated and washed twice in succession with 200 mL of distilled water, 200 mL of 30 % HCl, and 200 mL of ethanol (after each wash-process, the material was filtered under vacuum). Then, the material was coagulated with 200 mL of ether, and the resulting suspension was filtered under vacuum. Finally, the solid obtained was re-dispersed into 200 mL of ethanol, filtered and vacuum-dried overnight at room temperature prior to characterization by XRD, FTIR-

ATR, XPS and HRTEM. 6.2 g of material with a dull gray like appearance (not as shiny as the starting material) was obtained.

2.5. Functionalization and Exfoliation of GO with TEMPO using (Br-TEMPO): GOFT1 and GOFT2

The exfoliation and functionalization reaction of graphite oxide to obtain graphene oxide layers functionalized with TEMPO groups (GOFT) in the presence of Br-TEMPO (oxoammonium salt) was performed in a glass reactor equipped with a cooling jacket, a condenser and a magnetic stirrer. In order to study the exfoliation and functionalization level in respect to the concentration of oxoammonium salt used, the distribution of functional groups (TEMPO) on the graphene oxide, and their reinforcement effect into polymer nanofibers, we synthesized graphene oxide layers functionalized with TEMPO at two different TEMPO concentrations, described as GOFT1 and GOFT2. To obtain GOFT1, 0.5 g of GO was placed into the glass reactor in the presence of 2.6 g (0.025 mol) of triethylamine (Et_3N), and 60 mL of DMF (to improve the GO dispersion). The dispersion was sonicated during 30 min at 150 W. Then, the dispersion was vigorously stirred and a solution of 2.5 g of Br-TEMPO (0.010 mol) in 40 mL of DMF was added dropwise. The reaction was carried out at 2 °C under N_2 atmosphere for 4 h to insure functionalization. Functionalized and exfoliated graphene oxide layers were washed with clean DMF and filtered using a Nylon membrane of 0.2 μm under vacuum, and were dried overnight at room temperature prior to characterization by XRD, FTIR-ATR, XPS and HRTEM. To obtain GOFT2, 6.8 g (0.067 mol) of Et_3N and 5 g (0.021 mol) of Br-TEMPO were used under the same experimental procedure described above.

2.6. Preparation of Polymer Solution and Polymer-GOFT Dispersions by Electrospinning

A 7.5 % wt. Nylon 6 solution was prepared by dissolving the polymer overnight in HFIP. The polymer-GOFT dispersions were prepared by placing the GOFT in HFIP at 0.1, 0.5 and 1 % wt. with respect to the polymer, and sonicated using the ultrasonic processor previously described; the sonication procedure was carried out for 1 h in an ice bath to avoid excessive heat generated during the process, affording a black-ink like appearance dispersion. The polymer solution and the polymer-GOFT dispersions were electrospun with a voltage of +15 kV to the needle tip, while the negative electrode was set to an applied voltage of −15 kV to the collector. A 15 cm distance between the needle tip and the rotating collector was used to obtain the nanofibers, which were dried under vacuum for 24 h in the presence of P_2O_5 to remove any possible traces of residual moisture and solvents. The nonwoven mats were characterized by mechanical testing.

2.6.1. Tensile testing—The nonwoven mats were cut into a "dog-bone" shape with 0.03 mm thickness, 2.75 mm width at their narrowest point and a gauge length of 7.5 mm, and tested under a crosshead speed of 10 mm/min. At least five specimens were tested for tensile behavior and the average values are reported.

3. Results and discussion

GO was obtained by oxidizing graphite nanoplatelets using an improved Hummer's method reported by Marcano *et al.*[19] However, we slightly modified this methodology increasing the reaction time from 12 h to 24 h, thus increasing ~31 % (respect to the oxidized material obtained by Marcano *et al.*[19]) the amount of hydroxyl (-OH), epoxy (-O-), carbonyl (C=O) and carboxylate (O-C=O) groups present on the surface and edges of GO. Also, combining all percentages of oxidized material from GO, we obtained 90.6 % of oxidized carbon and 9.4 % of graphitic carbon, as demonstrated by XPS in another section of this paper.

3.1. Exfoliation/Functionalization

3.1.1 Proposed Mechanism—In order to study the exfoliation and functionalization level in respect to the concentration of oxoammonium salt (OS) used, we synthesized graphene oxide layers functionalized with TEMPO at two different concentrations, identified as GOFT1 and GOFT2. Although the structure of GO is still uncertain,[20] the presence of functional groups (OH, COOH, C=O and C-O-C) along their surface and edges is recognized.[19],[20] In addition, the molar concentration of these functional groups and their distribution strongly depends on the oxidation pathway used.[19],[21],[22]

Therefore, under the conditions used in this investigation, the protons in aromatic alcohol and acid moieties present on the surface and edges of GO should be first abstracted by an excess of phenoxides and carboxylates,[15] which then react with the Et_3N,[15],[23], resulting in 2,2,6,6,tetramethylpiperidine-1-oxonium cation to yield different functional groups. Furthermore, phenols are known to oxidize under free radical conditions[24] (TEMPO itself is a free radical[12]), so we speculate that the material obtained consists of GO with several functional groups and alkoxyamine species attached to it. Meanwhile, the bromine anion is capped with Et_3NH^+ forming a white precipitate, indicating that the reaction has taken place. Hence, the reaction with TEMPO seems to promote an oxidation of GO and a simultaneous exfoliation, as represented in Figure 1.

While the products of the material obtained are not clear at the present time, and are currently under investigation in our research group, there are several papers that suggest the feasibility of the proposed structure in Figure 1. For example, Liu *et al.*[25] reported the feasibility of oxidizing graphene oxide into graphene peroxide in the presence of oxygen using ^{60}Co γ-rays. The starting materials and the products were characterized by FTIR, Raman, XPS and XRD in an effort to elucidate the structure of the final product.

Further, the use of TEMPO as an oxidizing agent has been reported in several organic compounds. Iwabuchi *et al.*[26] reported the oxidative rearrangement of tertiary allylic alcohols to β-substituted α,β-unsaturated carbonyl compounds using oxoammonium salts (OS) in acetonitrile at room temperature. Semmelhack *et al.*[27] published the oxidation of primary and secondary alcohols using TEMPO through four different possible intermediates, one of which included the deprotonation of primary and secondary alcohols under basic conditions to afford hydroxyl radicals; the resulting products consisted of aldehydes and ketones and alkylated oxoammonium products, which resemble our proposed structures in Figure 1. Furthermore, Bailey *et al.*[15] performed a computational study on the oxidation of primary and secondary alcohols with TEMPO under basic conditions, where it was found that the first step of the reaction involved an alkoxide attack on the electrophilic nitrogen in TEMPO, affording aldehydes, ketones and TEMPO byproducts.

TEMPO has also been attached to inorganic particles. It was incorporated onto Fe_3O_4[18] and silica,[16] with both of these particles being subsequently reacted with styrene and maleic anhydride to produce a core inorganic nanoparticle with polymer chains extending from it. Therefore, these publications suggest that graphite oxide used under the conditions presented in this report could be oxidized to contain peroxides, aldehydes and ketones, as well as to the attachment of TEMPO to the surface of the starting material, as shown Figure 2.

The reaction presented in Figure 2 (Scheme 1) proposes a free radical oxidation mechanism of a simplified GO, which is based on the oxidation mechanism of phenols and hydroquinone[28],[29]. Thus, TEMPO abstracts in two steps the hydrogen atoms present in the alcohols, leaving behind a di-radical species that rearranges to afford ketones. In addition, Figure 2 (Scheme 2) proposes an oxidized product and the attachment of the

2,2,6,6,tetramethylpiperidine-1-oxonium by three different possible mechanisms. Path A and B utilize Et_3N in the first step to produce a phenoxide, which then can follow different routes. The phenoxide on path A can react with TEMPO in a single electron transfer process to afford a phenoxyl radical and a nitroxyl radical; subsequent oxidation of the phenoxyl radical yields an aryl radical that is scavenged by the nitroxyl radical, thus accounting for the formation of C-N bonds observed in XPS. Path B shows the phenoxide attack on the oxygen of TEMPO to produce an unstable peroxide which cleaves homolitically, and the resulting aryl radical rearranges and is scavenged by TEMPO. In a third possibility (path C), TEMPO does a single electron transfer (SET) to a phenol group, which then produces a radical species under basic conditions, followed by rearrangement and scavenging by TEMPO. It is important to note that the proposed pathways and mechanisms have been reported previously by several authors[27],[15],[30],[31],[32] for alcohols, but have not been set forth for graphite oxide.

Since GO can contain epoxides in its structure, Figure 3 addresses this possibility.

In this case, phenol is deprotonated in the presence of Et_3N resulting in a phenoxide, which attacks the 2,2,6,6,tetramethylpiperidine-1-oxonium cation to form a peroxide. Subsequently, the CO-ON bond cleaves to form an oxyl radical, which reacts intramolecularly to form a five member ring endo peroxide that contains an aryl radical, which is then scavenged by TEMPO. Finally, Figure 4 proposes that the carboxylic acid moieties found in GO react in an acid-base manner with Et_3N as the first step.

A nucleophilic attack on nitrogen (path D) will form an intermediate that will follow a Meisenheimer rearrangement to add TEMPO to its structure and release CO_2 as a byproduct. Nevertheless, if the attack occurs on oxygen (path E), a peroxide is formed and a radical mechanism is followed. The peroxide is cleaved and the resulting radical acid decomposes into CO_2 and an aryl radical, which is scavenged by TEMPO to produce an alkoxyamine.

3.1.2 Dispersion study—The highly oxidized layers of GO produced herein exhibited dispersions with long-term stability (3 weeks) in DMF, which is in good agreement with the literature.[33] So, this solvent promotes a better diffusion of reactive species between well dispersed GO layers during the functionalization reaction (4 h), enhancing its exfoliation. In addition, GOFT1 and GOFT2 were dispersed in DMF, H_2O DI, n-hexane, toluene, THF, $CHCl_3$, methanol, HFIP, acetone and CH_2Cl_2 (1 mg/mL) using an ultrasonication bath for 1 h. Figure 5 shows digital pictures of all dispersions sonicated at time 0 h. and after 72 h.

For the samples sonicated at 0 h., it can be noticed that GOFT1 could be dispersed in almost all of the solvents, except n-hexane, toluene, THF, and to a lesser extent in CH_2Cl_2. In contrast, GOFT2 could only be well dispersed in DMF, DI H_2O and HFIP. Many of these dispersions displayed only short-term stability and precipitated completely in a matter of hours to a few days. After sonication, GOFT1 remained dispersed for 72 h in HFIP, DMF and DI H_2O, and to a lesser degree in methanol. Meanwhile, GOFT2 showed a relatively good stability in HFIP, DMF and DI H_2O. GOFT1 exhibited a better dispersion after 72 h in DMF and HFIP than GOFT2. These results suggest that GOFT2 possess a different concentration or distribution of functional groupsTransmitance that reduce slightly its dispersion in HFIP. Thus, HFIP was used to disperse GOFT1 or GOFT2 into the polymer solution (Nylon 6/HFIP) to obtain composites of nonwoven mats by electrospinning.

3.2. Functionalized Graphene layers with TEMPO groups

GO, GOFT1 and GOFT2 were qualitatively analyzed and their structures evidenced by FTIR-ATR as shown in Figure 6.

Figure 6 shows characteristic vibrations of GO, which exhibits the following functional groups[19],[25]: O-H stretching vibrations (3420 cm^{-1}), C=O stretching vibration (1720–1740 cm^{-1}), C=C from unoxidized sp^2 bonds (1620–1640 cm^{-1}), and stretching vibrations (1103 cm^{-1}).[33] New vibrations at 2910–2971 cm^{-1} and 1362 cm^{-1} were observed in GOFT1 and GOFT2, which were attributed to CH_3, CH_2 and N-O stretching vibrations from the piperidine ring from TEMPO. Further, a new small vibration centered at 850 cm^{-1} was observed and attributed to a new peroxide bond[25] (in agreement with the proposed mechanism in Figure 3). Despite the fact that the O-O stretch occurs in the region where carbon skeletal vibrations modes may interfere, it has been demonstrated that the stretching vibrations of peroxide groups occur in a narrower interval of frequencies (845–875 cm^{-1}) [34], which can be distinguishable to the carbon skeletal vibrations modes.

3.3. GOFT1 and GOFT2, Exfoliation level

The level of exfoliation from GO to nitroxide-functionalized graphene oxide (GOFT1 and GOFT2) was analyzed by X-ray diffraction (XRD) as shown in Figure 7.

Pristine graphite (GN) presented its characteristic main peak (2θ Bragg angle) at 26.5° (Figure 7), indicating a highly organized layered structure.[35] In the case of GO, it is possible to observe a shift in the main peak (2θ Bragg angle) from 26.5° (corresponding to $d_{0001} = 0.34$ nm spacing between atomic planes in graphite), to 10.1° in GO (corresponding to an interplane distance of $d_{0001} = 0.94$ nm). This level of exfoliation (from $d_{0001} = 0.34$ nm to $d_{0001} = 0.94$ nm) is obtained when pristine graphite is oxidized using the modified Hummer's method.[19] The amount of OH and COOH groups capable of reacting with Br-TEMPO salt are determined by the oxidation process and it is likely that they are distributed predominantly on the edges.[20] The large amounts of the Br-TEMPO salt used to prepare GOFT1 or GOFT2 should saturate all possible reactive groups at the GO surface, so exfoliated individual functional graphene layers should be obtained in a single step. A shift and a decrease in the intensity of the Bragg peak up to 7.9° was observed, which corresponds to the spacing between atomic planes in graphite of $d_{0001} = 1.12$ nm. According to the mechanism proposed herein (see Figures 2–4), the functionalization/exfoliation reaction involves the oxidation of several groups and the formation of alkoxyamines. In conclusion, we believe that the oxidation promoted by OS and their corresponding functionalization with TEMPO groups at the GO edges originates an increase in the interplanar distance producing graphene oxide single layers decorated with TEMPO groups, causing the interplanar distance between layers to increase 0.18 nm in both functionalized materials (GOFT1 or GOFT2). In consequence, the surface of each new exfoliated layer is exposed and can react with the OS remaining, increasing the functional groups concentration, but not the interlayer spacing; this discussion is addressed by XPS in a subsequent section.

3.4. GOFT1 and GOFT2, Functionalization level

The percent of nitroxide chemically bonded to the graphene structure was determined using X-ray photoelectron spectroscopy (XPS) in GN, GO and GOFT samples. Figure 8 shows the XPS spectra.

Figure 8a corresponds to the precursor graphite, clearly showing a carbon sp^2 (C=C) peak near 284.5 eV.[36],[37] However, Figure 8b shows that the sp^2 carbon peak was significantly reduced in GO, and a new carbon sp^3 (C-C) peak at 285.1 eV was formed;[38],[39] also, new functional groups containing oxygen-related sp^2 carbon peaks were observed, which represents the formation of C-OH (hydroxyl) at 286.4 eV;[38],[39] C=O, C-O-C (carbonyl and epoxy) at 287.7 eV,[38] and COOH (carboxylic acid) at 288.9 eV.[25] Also, the π-plasmon peak (ascribed to $\pi-\pi^*$ shake-up transitions) near to 291 eV was observed,

[38],[39] which reveals aromatic ring structures attributed to exfoliated layers with low level of functional groups. The presence of sp^3-carbon and the high content of oxidized species demonstrate the change of graphite structure due to oxidation.

Interestingly, the samples functionalized with TEMPO groups (GOFT1 and GOFT2) in Figure 8c and Figure 8d, exhibited two new peaks centered at 285.2 eV[40] and 289.2 eV[25] respectively, which were attributed to the C-N bond corresponding to the piperidine ring from TEMPO (see Figure 2-Scheme 2) and at the new peroxide group (-O-O-) formed during functionalization (see Figure 3), correspondingly. Liu *et al.*[25] irradiated GO with ^{60}Coγ-rays and demonstrated the presence of peroxide groups C-O-O-H by XPS at 289.2eV. As discussed previously, we propose that peroxide groups are formed in the present studies during the functionalization and exfoliation process (Figure 4), so the proposed mechanism correlates with the XPS and FTIR data. Furthermore, COOH groups are present in GO (Figure 8b), but their presence after the reaction was not observed (Figures 8c and 8d). Therefore, this evidence also supports the mechanism proposed in Figure 4, where the COOH groups react with the Br-TEMPO salt forming CO_2 and alkoxyamine species. Finally, the π-plasmon peak[39] was observed in the spectrum. Table 1 reveals the percent composition obtained by integrating the deconvoluted curves for each sample.

In the case of GOFT1, Table 1 reveals an increase of ~ 9.2 % (respect to GO) in C-sp^3, which is congruent with the percent amount of new C-N bond found of 9.5 %, which was attributed to the presence of the new TEMPO groups chemically attached onto the graphene layers. Also, a decrease of OH and an increase of C=O groups (both in respect to GO) of about 15 % and 9.6 % respectively were observed. In addition, COOH groups (3.7 % in GO) were not observed in the functionalized materials, while the new peroxide bonds (4.6 %) were observed. The new percent composition of C-N bond is formed by the modification of: i) 3.7 % (functionalization and loss of COOH); ii) 4.6 % (oxidation/functionalization of OH groups nearest to an oxirane ring), and iii) 1.2 % (oxidation/functionalization of OH groups). Meanwhile, – OH groups (15 %) are consumed as follow: 4.6 % to produce O-O, 1.2 % reacts with OS to leads alkoxyamine and C=O, and 8.4 % is oxidized to C=O. Finally, 9.6 % of C=O is obtained by the modification of 8.4 % (oxidation of – OH to C=O) and 1.2 % during the oxidation/functionalization of – OH groups to C=O and alkoxyamine. Thus, we find that GOFT1 was oxidized ~ 25.8 % more than GO. This explains why the interplanar distance between functionalized layers (measured by XRD analysis) was increased up to d_{0001} = 1.12 nm.

In the case of GOFT2, an increase of about 10.5 % and 5.9 % of OH and C=O groups (both in respect to GOFT1) was found respectively. Therefore, OH groups (10.5 %) are consumed as follows: 0.3 % to produce O-O, 5.1 % reacts with OS to lead alkoxyamine and C=O, and 0.8 % is oxidized to C=O. The new percent composition of the C-N bond was practically the same than in GOFT1. Finally, 5.9 % of C=O was obtained by the contribution of 0.8 % (oxidation of OH to C=O) and 5.1 % during the oxidation/functionalization of OH groups to C=O and alkoxyamine. In this case, GOFT2 was slightly more oxidized than GOFT1. Although GOFT1 and GOFT2 exhibited the same shift in XRD, and exhibited the same C-N percentage value in XPS, we argue that the amount of OS used in each system was enough to saturate all possible reactive groups atXPS Intensity (a.u.) the edges of GO as to produce an exfoliation. Nonetheless, the surface of each new exfoliated layer could react with the OS remaining, slightly increasing the oxidation level. On this basis, we could assume that GOFT2 layers will exhibit a more amorphous surface than in GOFT1, as will be demonstrated by HRTEM later.

Moreover, Choi *et al.*[41] doped epitaxial graphene with nitroxide groups (4-amino-TEMPO) and observed by N1s XPS a N-O bond centered at 406 eV. In this study, the N-O bond for GOFT1 and GOFT2 was observed (as revealed in Figure 9) by N1s XPS at the same binding energy as reported in the literature.[41]

3.5. GOFT1 Morphology by HRTEM

GO and GOFT1 were characterized by high-resolution transmission electron microscopy (HRTEM) as shown in Figure 10. Each sample was dispersed into methanol and one drop was placed onto a copper grid with an ultrathin holey carbon film.

Figure 10a shows an image of GO at low magnification. In general, GO tends to congregate to form multilayer agglomerates that result in tens or several hundreds of nm^2. In particular, we observed the presence of a fracture line on the layers, which we attribute to the oxidation process. Figure 10b shows an image of GO at high magnification, which illustrates the amorphous zones of GO with numerous wrinkles. The diffraction rings of a selected area electron diffraction (SAED) is the inset in Figure 10b, where a hexagonal symmetry with diffused diffraction spots is observed, confirming the amorphous structure of GO; although it is possible to observe small domains of around 2 nm of crystalline patterns on the edges in the stack.

Figure 10c corresponds to GOFT1 showing a single-layer of graphene functionalized with TEMPO moieties, having sizes of several hundreds of nm^2. The fracture-line of the layer caused during the oxidation of graphite was also observed. Figure 10d shows an image at high magnification corresponding to GOFT1 with well-defined amorphous and crystalline zones like "islands" (circumscribed in red circles) on the surface of the graphene layer, and which are attributable to oxygen-free regions.[42] This is in agreement with our XPS results, being that in the functionalized samples a π-plasmon peak was observed and attributed to aromatic ring structures. SAED (inset) pattern shows that {0–110} and {−1010} spots appear to be more intense than {1–210} and {−2110} spots, which is the fingerprint of single-layer of graphene. In order to demonstrate this, the intensity of each spot was studied as a function of different tilts in respect to the incident beam for the sample GOFT1. According to Meyer *et al.*[42],[43] for a monolayer of graphene, the spots intensity at {0–110} and {−1010} should remain constant as the sample is tilted. Figure 10e shows an example of SAED at 8° of tilt, which demonstrated that the intensity of the {1–210} diffracted spot, is considerably lower than the {0–110} spot. Finally, Figure 10f reveals the intensities ratio between {0–110}/{1–210} and {−1010}/{−2110} spots in respect to the tilt, and confirms the presence of a single-layer of graphene functionalized with TEMPO. GOFT2 also was analyzed by HRTEM as shown in Figure 11.

Figure 11 did not present crystalline zones, only an amorphous structure was observed along the surface and edges due to the high amount of C-sp^3 new bonds, which is in agreement with the functionalization reaction proposed and the percent composition by XPS obtained. Also SAED (inset) pattern shows {0–110} and {−1010} spots more intense than {1–210} and {−2110} spots, which confirm the fingerprint of single-layer of graphene in GOFT2.

3.5.1 Morphology by SEM—Scanning Electron Microscopy (SEM) was performed to confirm the morphology of the nanofibers containing GOFT1 and GOFT2, as shown in Figure 12. It can be observed that these materials are defect free (no beads or beads on string morphology) with regular and homogeneous surfaces.

It is noted that the nanofibers containing GOFT1 possess a more homogeneous distribution of fibers diameters than GOFT2; however, the average fiber diameter for GOFT1 was of 400 ± 100 nm, while GOFT2 exhibited an average fiber diameter of 200 ± 100 nm. This

difference can be attributed to the dispersion state of GOFT1 and GOFT2 in HFIP. According to the dispersion study (see 3.1.2 Section), GOFT1 exhibits stable dispersions up to 72 h in HFIP, which promotes the formation of more homogeneous nanofibers during the electrospinning process. In contrast, the dispersions containing GOFT2 are not stable, so it is possible that some re-agglomeration of the nanoparticles occurs. As a consequence, different concentrations of GOFT2 are expected within the nanofibers obtained, thus promoting more heterogeneity in fibers diameters.

3.6. Mechanical Properties of new Composites based on GOFT1 and GOFT2 with Nylon 6 nanofibers

The newly synthesized GOFT1 and GOFT2, which are exfoliated and possesses nitroxide groups, should allow better dispersion and compatibility with a polymer matrix, significantly improving the final properties of the composite material. In order to demonstrate this hypothesis, we dispersed 0.1, 0.5 and 1 wt.% of GOFT1, GOFT2, GO and GN in Nylon 6 through ultrasound. The resulting dispersions were electrospun to obtain non-woven nanofibers composites with 0.03 mm of thickness. Tensile testing[44],[45],[46] was performed on these samples and the tensile stress, tensile strain and Young's modulus were determined.

Figure 13 shows a 3D graph of the mechanical properties obtained for each system at the concentrations aforementioned, while Table 2 shows the absolute values of tensile stress, tensile strain and Young's modulus of each sample. Figure 13 demonstrates that pristine Nylon 6 has a relatively low tensile stress and strain, and a moderate Young's modulus. Although addition of GN and GO moderately enhance these properties at different concentrations, GOFT1 at 0.1% wt. increases simultaneously all of them, 95% tensile strength, 73% Young's modulus and 82% tensile strain in respect to Nylon 6 nanofibers. This is a significant result, not only because of the magnitude of the enhancement on the mechanical properties, but also because the usual effect is that one of these properties increases at the expense of another in polymeric systems,[47] and in graphene paper[48]. It is interesting to note that the Nylon 6 nanofibers containing the lowest concentration of GOFT1 (0.1 % wt) reached the most significant enhancement in mechanical properties. Further addition of GOFT1 within the nanofibers was detrimental to the properties investigated, and the possible causes for this effect will be reported elsewhere. The area of influence of GOFT1 is indicated in Figure 13, where it is evident that the material presents potential applications as an additive for polymer matrices.

On the other hand, although GOFT1 and GOFT2 exhibited the same amount of nitroxide (C-N ~ 9.1 – 9.5 %) by XPS and the same interplanar distance by XRD (d_{0001} = 1.12 nm), the mechanical behavior is different at the same weight percent. As already discussed, it is possible that the slightly more oxidized (0.8 %) GOFT2 re-agglomerates, producing a different mechanical behavior, which is not ascribable to the TEMPO loading.

4. Summary

In summary, a facile strategy to obtain exfoliated and functionalized graphene oxide with TEMPO groups from graphite oxide using oxoammonium salts (OS) in a one pot step has been demonstrated for the first time. Also, highly oxidized graphite oxide (GO, 90.6 % of oxidized carbon) was obtained, modifying the reaction time in the strategy proposed by Marcano *et al.*[19] Two functionalized graphene layers were produced herein (GOFT1 and GOFT2) and the mechanisms of functionalization/exfoliation were proposed, where the oxidation of phenols to ketone groups, the rearrangement of epoxides and carboxylic acids, and the formation of alkoxyamine species are suggested. Both functionalized materials exhibited a shift and broadening of the Bragg peak up to 7.9° corresponding to an interlayer

spacing of $d_{0001} = 1.12$ nm. A new C-N and peroxide O-O bonds were confirmed by C1s XPS corresponding to the piperidine ring from TEMPO and the peroxide bonds. Using low amounts of OS (GOFT1 strategy), it was possible to obtain functionalized graphene layers with amorphous and crystalline zones at a 50:50 ratio, which was confirmed by HRTEM obtaining their fingerprint by electron diffraction at several tilts. The potential use of these materials within polymer matrices was confirmed, where the tensile stress, tensile strain and Young's modulus were simultaneously increased ~ 100 % in respect to pristine Nylon 6 when the functionalized/exfoliated GOFT1 (low concentration of nitroxide groups) was used. ACKNOWLEDGMENT

Acknowledgments

References

1. Geim AK, Novoselov KS. The rise of graphene. Nat Mater. 2007; 6(3):183–91. [PubMed: 17330084]

2. Balandin AA. Thermal properties of graphene and nanostructured carbon materials. Nat Mater. 2011; 10(8):569–81. [PubMed: 21778997]

3. Zhang Y, Tan Y-W, Stormer HL, Kim P. Experimental observation of the quantum Hall effect and Berry's phase in graphene. Nature. 2005; 438(7065):201–4. [PubMed: 16281031]

4. Gomes KK, Mar W, Ko W, Guinea F, Manoharan HC. Designer Dirac fermions and topological phases in molecular graphene. Nature. 2012; 483(7389):306–10. [PubMed: 22422264]

5. Lee C, Wei X, Kysar JW, Hone J. Measurement of the Elastic Properties and Intrinsic Strength of Monolayer Graphene. Science. 2008; 321(5887):385–8. [PubMed: 18635798]

6. Novoselov KS, Geim AK, Morozov SV, Jiang D, Zhang Y, Dubonos SV, et al. Electric Field Effect in Atomically Thin Carbon Films. Science. 2004; 306(5696):666–9. [PubMed: 15499015]

7. Sutter PW, Flege J-I, Sutter EA. Epitaxial graphene on ruthenium. Nat Mater. 2008; 7(5):406–11. [PubMed: 18391956]

8. Park S, Ruoff RS. Chemical methods for the production of graphenes. Nat Nano. 2009; 4(4):217–24.

9. Wan X, Huang Y, Chen Y. Focusing on Energy and Optoelectronic Applications: A Journey for Graphene and Graphene Oxide at Large Scale. Acc Chem Res. 2012; 45(4):598–607. [PubMed: 22280410]

10. Georgakilas V, Otyepka M, Bourlinos AB, Chandra V, Kim N, Kemp KC, et al. Functionalization of Graphene: Covalent and Non-Covalent Approaches, Derivatives and Applications. Chem Rev. 2012; 112(11):6156–214. [PubMed: 23009634]

11. Bonilla-Cruz, J.; Dehonor, M.; Saldívar-Guerra, E.; González-Montiel, A. Polymer Modification: Functionalization and Grafting. In: Saldivar-Guerra, E.; Vivaldo-Lima, E., editors. Handbook of Polymer Synthesis, Characterization, and Processing. Wiley; 2013. p. 205-23.

12. Grubbs RB. Nitroxide-Mediated Radical Polymerization: Limitations and Versatility. Polym Rev. 2011; 51(2):104–37.

13. Nilsen A, Braslau R. Nitroxide decomposition: Implications toward nitroxide design for applications in living free-radical polymerization. J Polym Sci Part A: Polym Chem. 2006; 44(2): 697–717.

14. Bobbitt JM. Oxoammonium Salts. 6.1 4-Acetylamino-2,2,6,6-tetramethylpiperidine-1-oxoammonium Perchlorate: A Stable and Convenient Reagent for the Oxidation of Alcohols. Silica Gel Catalysis. J Org Chem. 1998; 63(25):9367–74.

15. Bailey WF, Bobbitt JM, Wiberg KB. Mechanism of the Oxidation of Alcohols by Oxoammonium Cations. J Org Chem. 2007; 72(12):4504–9. [PubMed: 17488040]

16. Bonilla-Cruz J, Lara-Ceniceros T, Saldívar-Guerra E, Jiménez-Regalado E. Towards Controlled Graft Polymerization of Poly [styrene-co-(maleic anhydride)] on Functionalized Silica Mediated by Oxoaminium Bromide Salt. Facile Synthetic Pathway Using Nitroxide Chemistry. Macromol Rapid Commun. 2007; 28(13):1397–403.

17. Bonilla-Cruz J, Lara-Ceniceros TE, Ramírez-Wong DG, Saldívar-Guerra E, Pérez-Rodríguez F, Márquez-Lamas U. Amphiphilic Block Copolymer from Hydroxyl-Terminated Polymers Functionalized with TEMPO. A New Synthetic Method Using Oxoammonium Salt. Macromol Chem Phys. 2011; 212:1654–62.

18. Chen F, Cai Z, Huang Y, Luo W, Chen J. Synthesis and characterization of copolymer grafted magnetic nanoparticles via surface-initiated nitroxide-mediated radical polymerization. Polym Eng & Sci. 2012; 53(5):956–62.

19. Marcano DC, Kosynkin DV, Berlin JM, Sinitskii A, Sun Z, Slesarev A, et al. Improved synthesis of graphene oxide. ACS nano. 2010; 4(8):4806–14. [PubMed: 20731455]

20. Dreyer DR, Park S, Bielawski CW, Ruoff RS. The chemistry of graphene oxide. Chem Soc Rev. 2010; 39(1):228–40. [PubMed: 20023850]

21. Hummers WS, Offeman RE. Preparation of Graphitic Oxide. J Am Chem Soc. 1958; 80(6):1339.

22. Shen J, Hu Y, Shi M, Lu X, Qin C, Li C, et al. Fast and Facile Preparation of Graphene Oxide and Reduced Graphene Oxide Nanoplatelets. Chem Mater. 2009; 21(15):3514–20.

23. Prucker O, Rühe J. Polymer Layers through Self-Assembled Monolayers of Initiators. Langmuir. 1998; 14(24):6893–8.

24. Tebben L, Studer A. Nitroxides: Applications in Synthesis and in Polymer Chemistry. Angew Chem Int Ed. 2011; 50(22):5034–68.

25. Liu J, Chen C, He C, Zhao J, Yang X, Wang H. Synthesis of Graphene Peroxide and Its Application in Fabricating Super Extensible and Highly Resilient Nanocomposite Hydrogels. ACS Nano. 2012; 6(9):8194–202. [PubMed: 22917015]

26. Shibuya M, Tomizawa M, Iwabuchi Y. Oxidative Rearrangement of Tertiary Allylic Alcohols Employing Oxoammonium Salts. J Org Chem. 2008; 73(12):4750–2. [PubMed: 18500838]

27. Semmelhack MF, Schmid CR, Cortés DA. Mechanism of the oxidation of alcohols by 2,2,6,6-tetramethylpiperidine nitrosonium cation. Tetrahedron Lett. 1986; 27(10):1119–22.

28. Lee CW, Jin SH, Yoon KS, Jeong HM, Chi K-W. Efficient oxidation of hydroquinone and alcohols by tailor-made solid polyaniline catalyst. Tetrahedron Lett. 2009; 50(5):559–61.

29. Sundaram S, Annamalai SK. Selective immobilization of hydroquinone on carbon nanotube modified electrode via phenol electro-oxidation method and its hydrazine electro-catalysis and Escherichia coli antibacterial activity. Electrochimica Acta. 2012; 62(0):207–17.

30. Ren T, Liu Y-C, Guo Q-X. Selective Oxyfunctionalization of Ketones Using 1-Oxopiperidinium Salt. Bull Chem Soc J. 1996; 69(10):2935–41.

31. Steenken S, Neta P. Electron transfer rates and equilibriums between substituted phenoxide ions and phenoxyl radicals. J Phys Chem. 1979; 83(9):1134–7.

32. Rhile IJ, Mayer JM. One-Electron Oxidation of a Hydrogen-Bonded Phenol Occurs by Concerted Proton-Coupled Electron Transfer. J Am Chem Soc. 2004; 126(40):12718–9. [PubMed: 15469234]

33. Paredes JI, Villar-Rodil S, Martínez-Alonso A, Tascón JM. Graphene Oxide Dispersions in Organic Solvents. Langmuir. 2008; 24(19):10560–4. [PubMed: 18759411]

34. Vacque V, Sombret B, Huvenne JP, Legrand P, Suc S. Characterisation of the O-O peroxide bond by vibrational spectroscopy. Spectrochimica Acta Part A: Molecular and Biomolecular Spectroscopy. 1997; 53(1):55–66.

35. Meng L-Y, Park S-J. Effect of exfoliation temperature on carbon dioxide capture of graphene nanoplates. J Coll Int Sci. 2012; 386(1):285–90.

36. Jeong H-K, Colakerol L, Jin MH, Glans P-A, Smith KE, Lee YH. Unoccupied electronic states in graphite oxides. Chem Phys Lett. 2008; 460(4–6):499–502.

37. Xu H, Suslick KS. Sonochemical Preparation of Functionalized Graphenes. J Am Chem Soc. 2011; 133(24):9148–51. [PubMed: 21604712]

38. Haubner K, Murawski J, Olk P, Eng LM, Ziegler C, Adolphi B, et al. The Route to Functional Graphene Oxide. ChemPhysChem. 2010; 11(10):2131–9. [PubMed: 20491134]

39. Meihua J, Hae-Kyung J, Tae-Hyung K, Kang Pyo S, Yan C, Woo Jong Y, et al. Synthesis and systematic characterization of functionalized graphene sheets generated by thermal exfoliation at low temperature. J Phys D: Appl Phys. 2010; 43(27):275402.

40. Amarnath CA, Hong CE, Kim NH, Ku B-C, Lee JH. Aniline- and N,N-dimethylformamide-assisted processing route for graphite nanoplates: intercalation and exfoliation pathway. Mat Lett. 2011; 65(9):1371–4.

41. Choi J, Lee H, Kim K-j, Kim B, Kim S. Chemical Doping of Epitaxial Graphene by Organic Free Radicals. J Phys Chem Lett. 2009; 1(2):505–9.

42. Meyer JC, Geim AK, Katsnelson MI, Novoselov KS, Booth TJ, Roth S. The structure of suspended graphene sheets. Nature. 2007; 446(7131):60–3. [PubMed: 17330039]

43. Meyer JC, Geim AK, Katsnelson MI, Novoselov KS, Obergfell D, Roth S, et al. On the roughness of single- and bi-layer graphene membranes. Solid State Commun. 2007; 143(1–2):101–9.

44. Jha BS, Colello RJ, Bowman JR, Sell SA, Lee KD, Bigbee JW, et al. Two pole air gap electrospinning: Fabrication of highly aligned, three-dimensional scaffolds for nerve reconstruction. Acta Biomaterialia. 2011; 7(1):203–15. [PubMed: 20727992]

45. Sell SA, McClure MJ, Ayres CE, Simpson DG, Bowlin GL. Preliminary Investigation of Airgap Electrospun Silk-Fibroin-Based Structures for Ligament Analogue Engineering. J Biomater Sci, Polym Ed. 2011; 22(10):1253–73.

46. Carrizales C, Pelfrey S, Rincon R, Eubanks TM, Kuang A, McClure MJ, et al. Thermal and mechanical properties of electrospun PMMA, PVC, Nylon 6, and Nylon 6,6. Polym Adv Tech. 2008; 19(2):124–30.

47. Wu G, Li H, Wu Y, Cuculo JA. Structure and property studies of poly(trimethylene terephthalate) high-speed melt spun fibers. Polymer. 2002; 43(18):4915–22.

48. Ranjbartoreh AR, Wang B, Shen X, Wang G. Advanced mechanical properties of graphene paper. J Appl Phys. 2011; 109(1):014306–12.
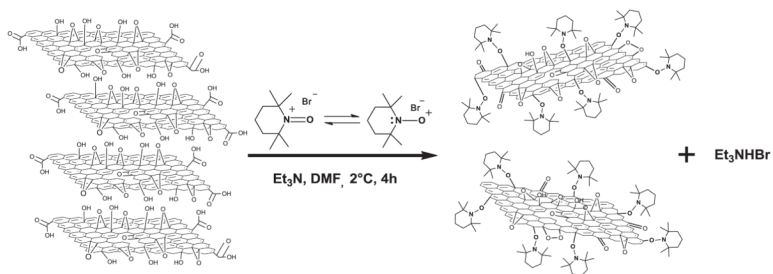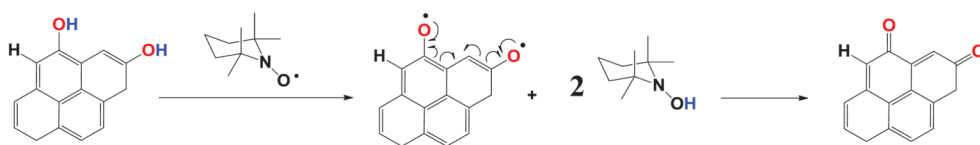
Figure 1.
General procedure of exfoliation and functionalization of GO using OS (Br-TEMPO).
Schematic representation.

Scheme 1
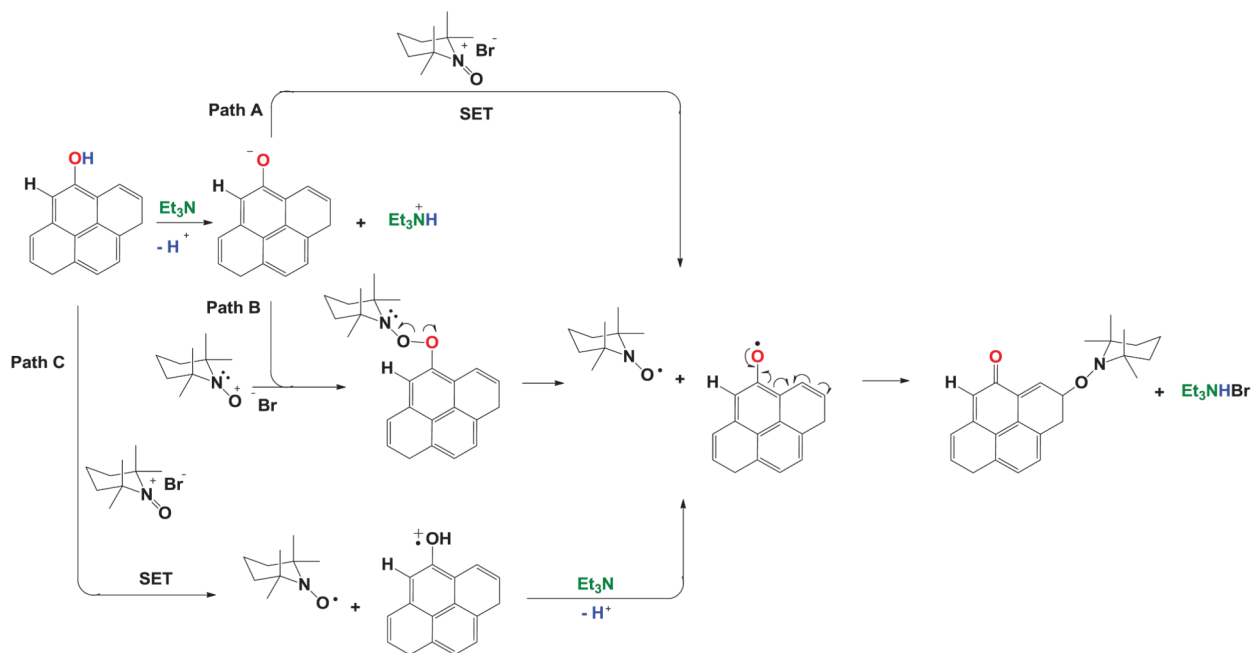

Scheme 2

Figure 2.
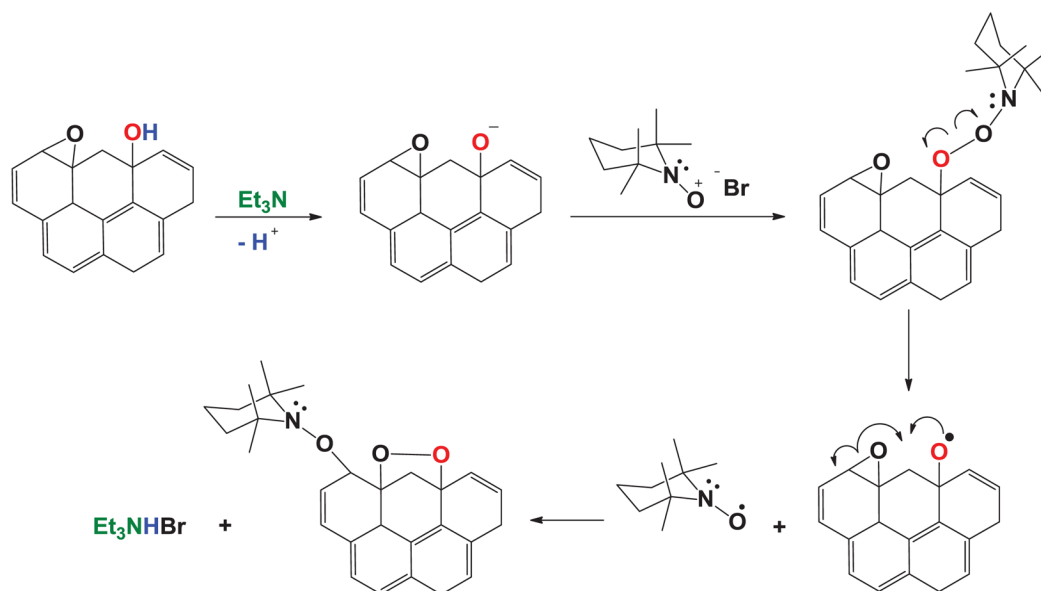Plausible reaction pathways and mechanisms during GO reaction with Br-TEMPO.
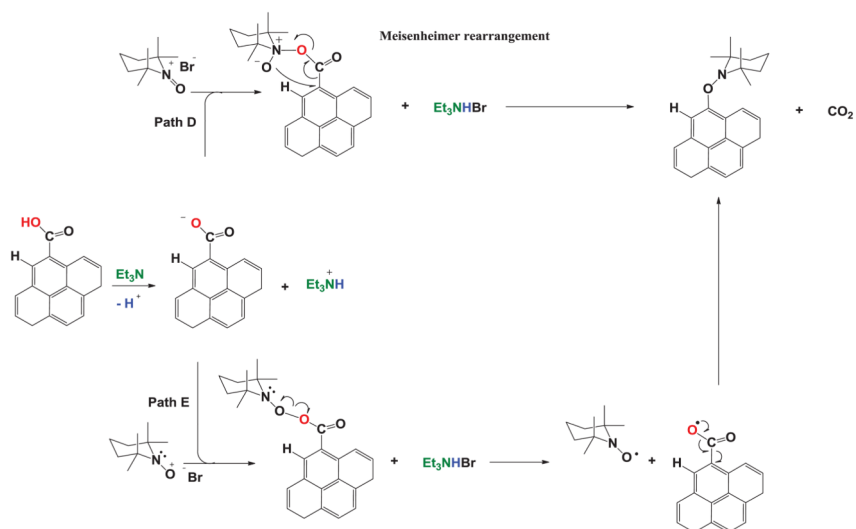
Figure 3.
Addition of TEMPO to epoxides in GO.
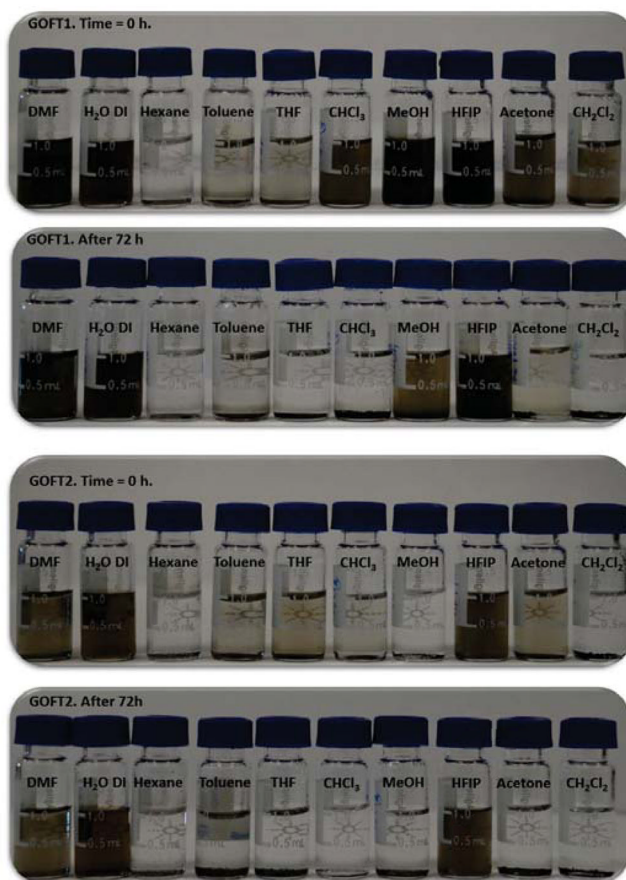
Figure 4.
Carboxylic acid reaction with TEMPO.

Figure 5.
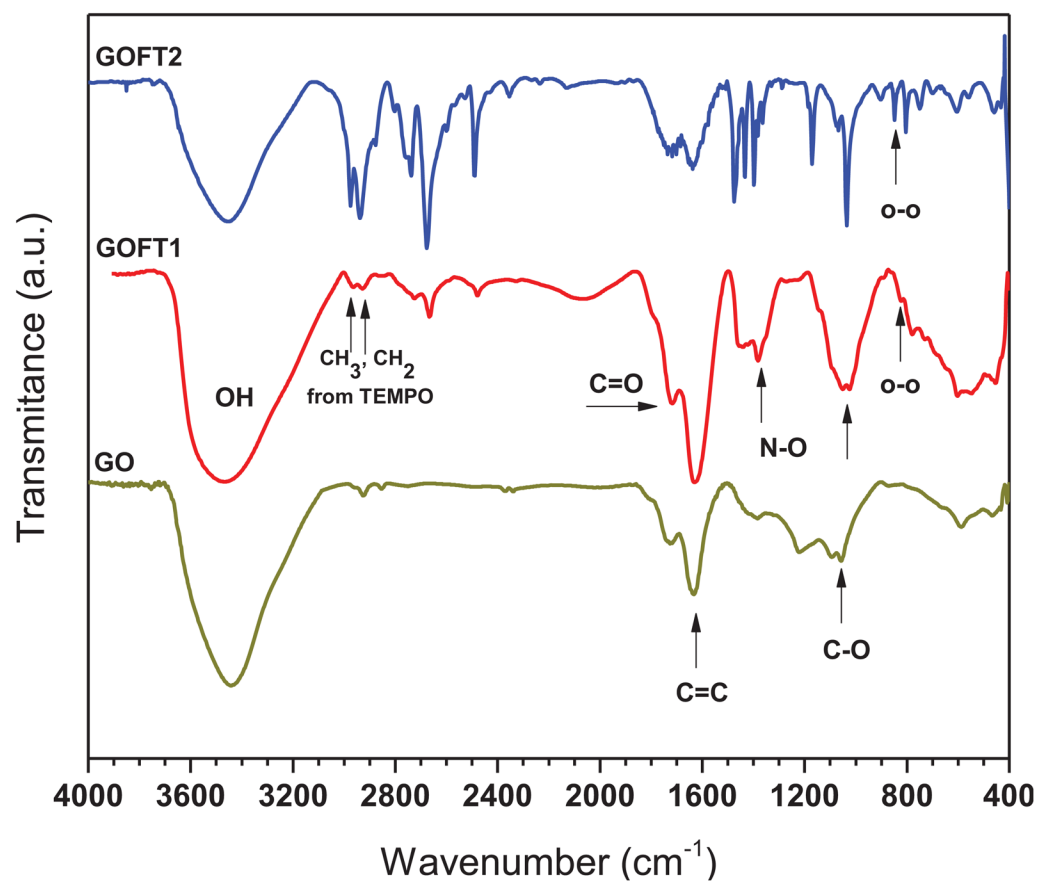Digital pictures of GOFT1 and GOFT2 dispersed in deionized water and 9 organic solvents.

Figure 6.
FTIR-ATR spectra of GO, GOFT1 and GOFT2
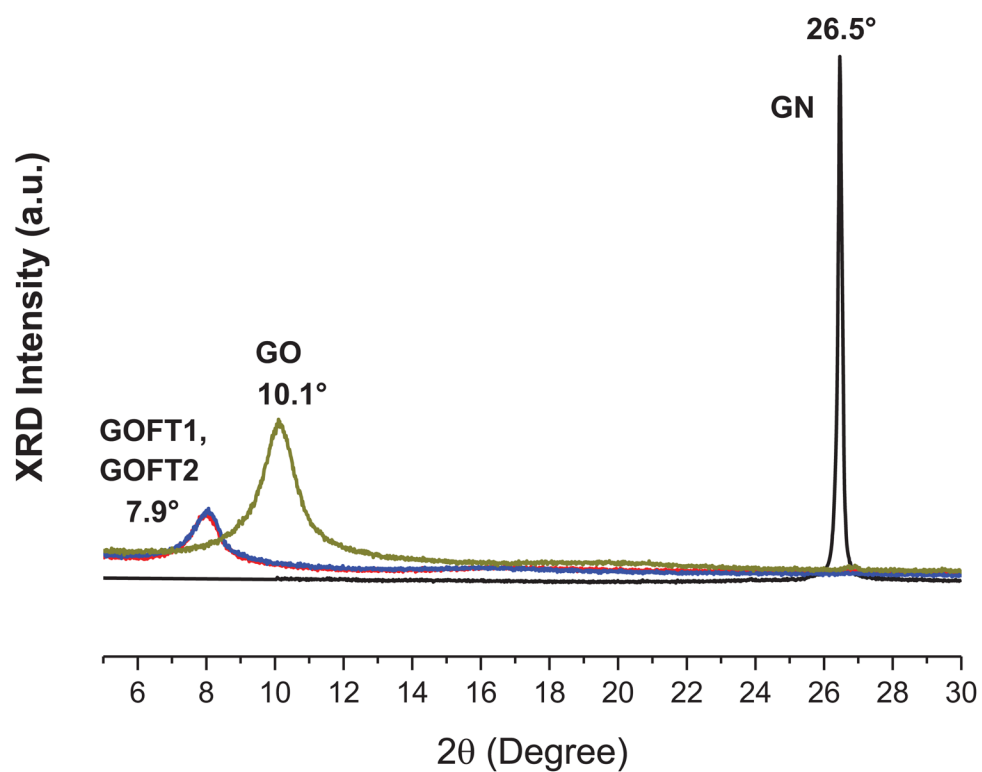
Figure 7.
XRD of pristine graphite (GN), graphite oxide (GO) and graphene oxide functionalized/
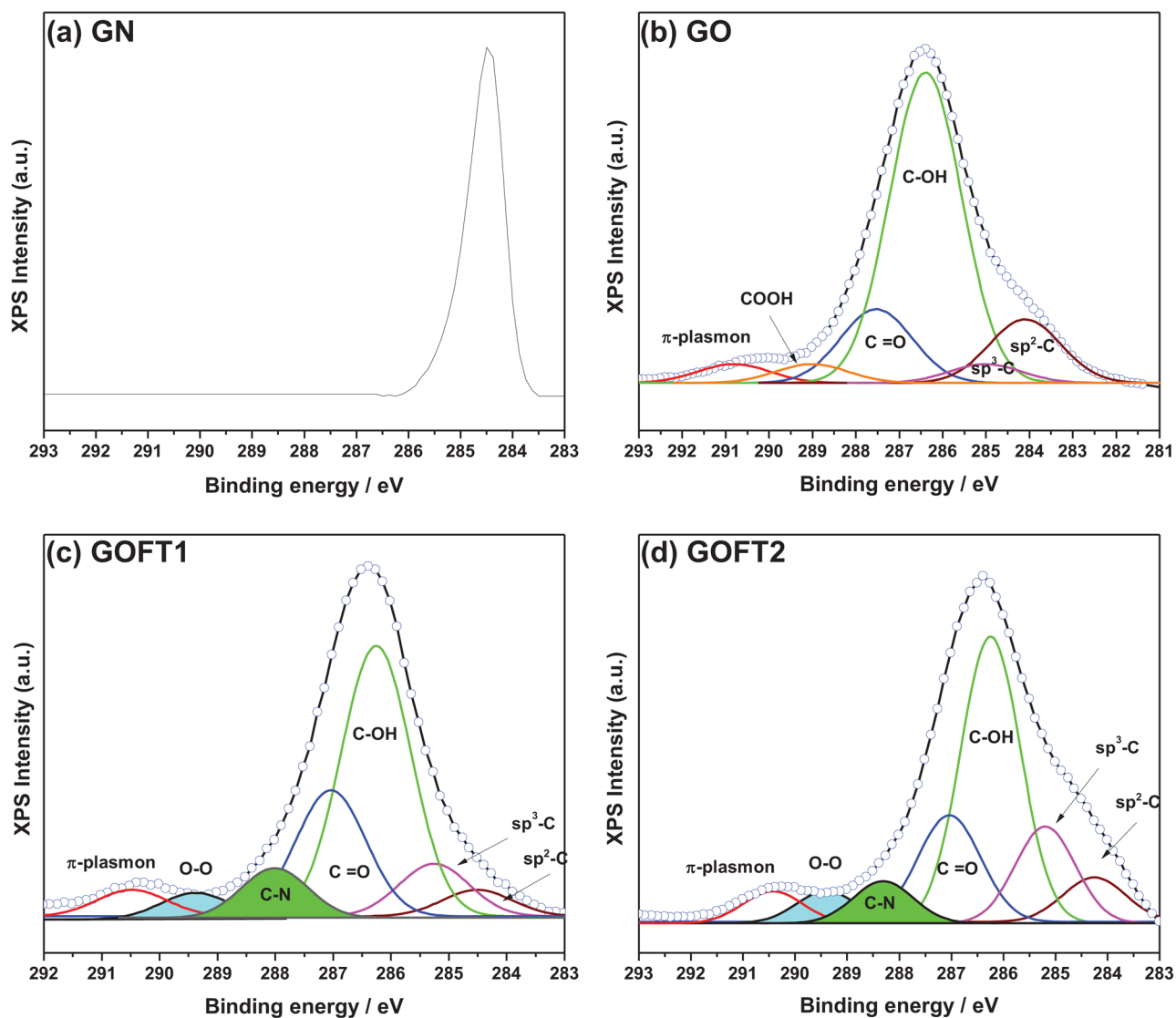exfoliated with TEMPO groups (GOFT).

Figure 8.
C1s XPS of: **a)** pristine graphite (GN), **b)** graphite oxide (GO), **c)** and **d)** graphene oxide functionalized with TEMPO groups using 0.01 mol and 0.02 mol of Br-TEMPO salt, respectively.
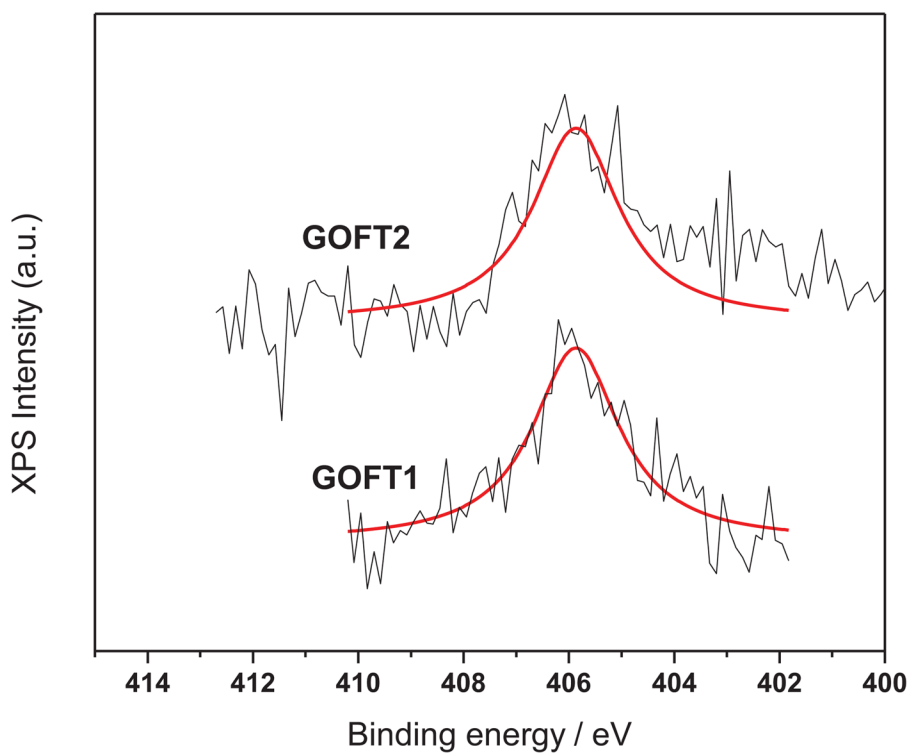
Figure 9.
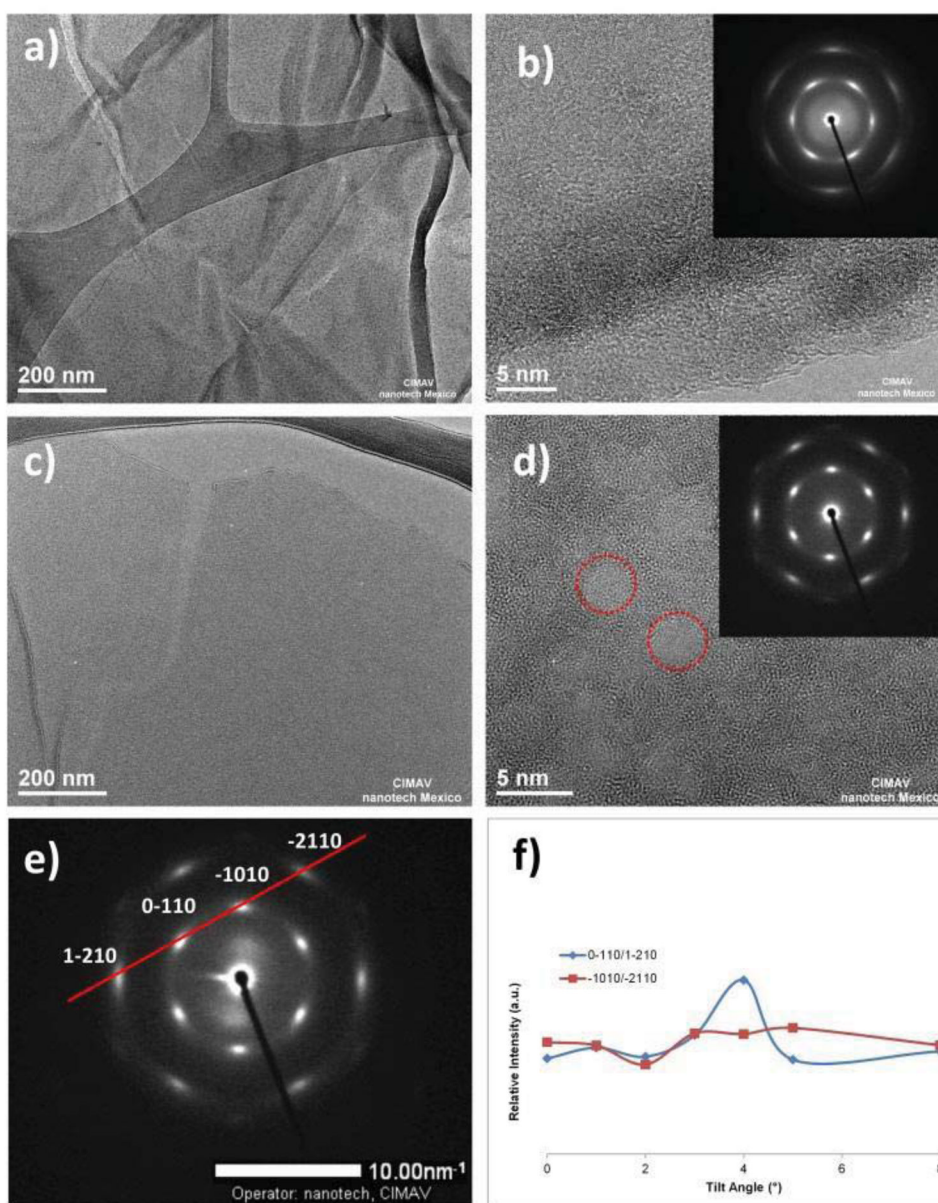N1s-XPS spectra for GOFT1 and GOFT2. N-O bond at 406 eV

Figure 10.
a) Low-magnification HRTEM image of GO exhibiting typical wrinkles in most of sheets;
b) High-magnification HRTEM image of GO showing amorphous and crystalline zones; **c)**
Low-magnification HRTEM image of GOFT1 showing a single layer of graphene-
functionalized; **d)** High-magnification HRTEM image of GOFT1 exhibiting amorphous and
crystalline zones; **e)** SAED from GOFT tilted 8° respect to the incident beam, showing a
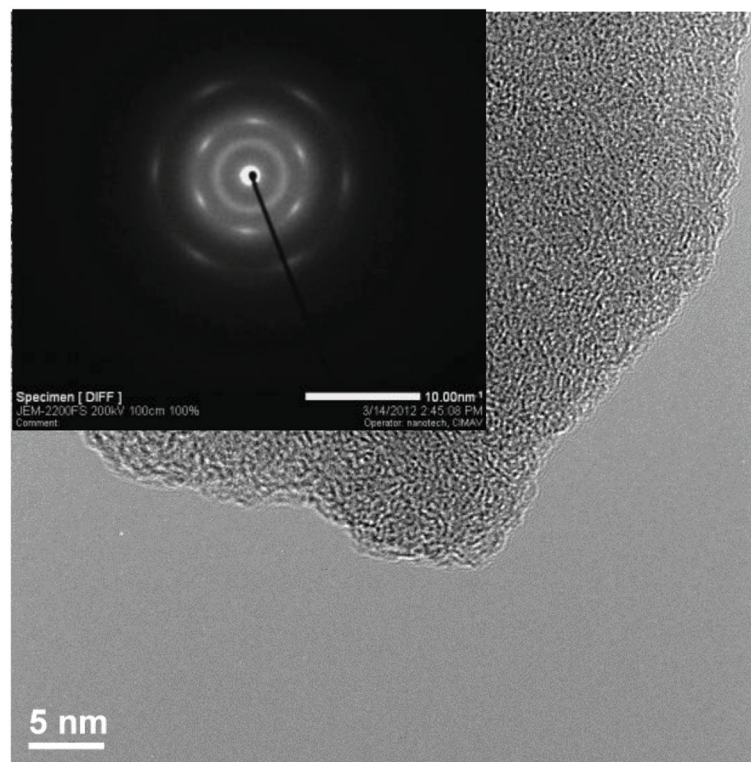hexagonal symmetry; and **f)** Spots intensities ratio at several tilts from GOFT1.

Figure 11.
HRTEM of GOFT2

Figure 12.
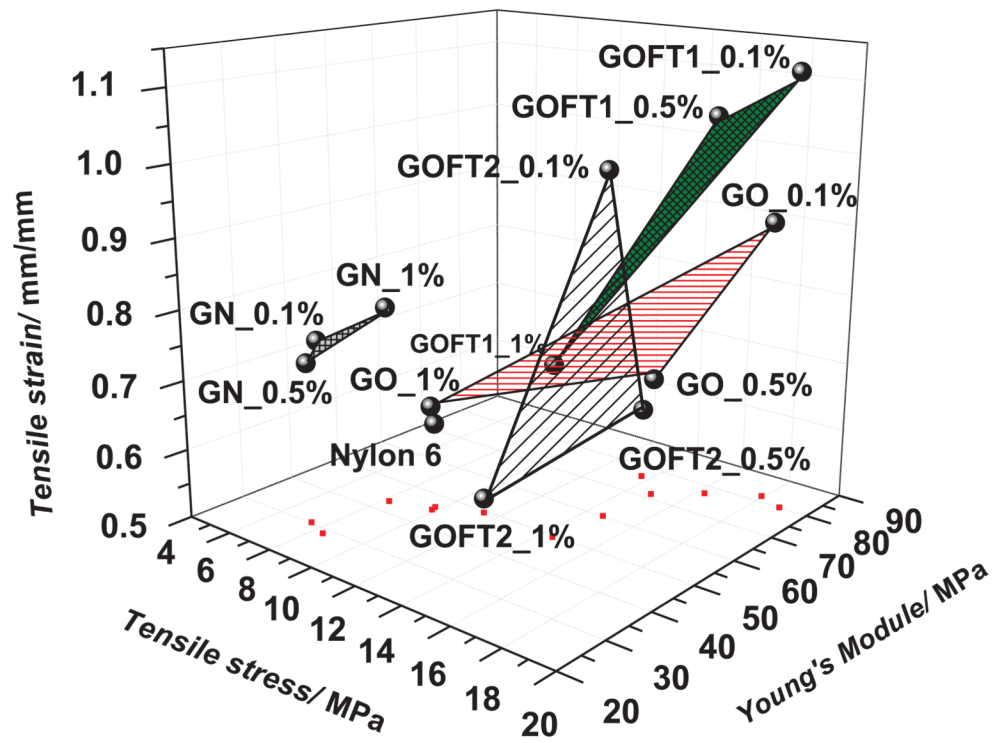SEM of Nylon 6 nanofibers containing GOFT1 and GOFT2

Figure 13.
Mechanical properties of Nylon 6 nanofibers and the corresponding composites containing GN, GO, GOFT1 and GOFT2. Red dots represent projections of each experimental point onto the XY plane.

Table 1

GO, GOFT1 and GOFT2 percent composition by C1s XPS

	C-sp^2	C-sp^3	C-OH	C=O	C-N	COOH	O-O	π–π*
GO	16.9	2.8	58	15	-	3.7	-	3.6
GOFT1	2.7	12	43	24.6	9.5	-	4.6	3.6
GOFT2	9.2	11.9	32.5	30.5	9.1	-	4.3	2.5

Table 2

Mechanical properties of nanofibers based on Nylon 6, and Nylon 6 reinforced with GN, GO, GOFT1 and GOFT2 at 0.1, 0.5 and 1 wt.%

	Tensile Stress (MPa)	Young's Modulus (MPa)	Tensile Strain (mm/mm)
Nylon 6	9.7	46.2	0.61
GN_0.1%	8.4	28.7	0.77
GN_0.5%	7.4	30.2	0.73
GN_1%	8.2	43.2	0.78
GO_0.1%	17.9	82.0	0.90
GO_0.5%	14.8	71.5	0.67
GO_1%	9.8	45.2	0.65
GOFT1_0.1%	18.91	80.1	1.11
GOFT1_0.5%	16.26	77.1	1.05
GOFT1_1%	14.43	49.4	0.84
GOFT2_0.1%	14.67	60.1	0.99
GOFT2_0.5%	13.63	76.4	0.60
GOFT2_1%	11.38	49.5	0.52